Available online at www.sciencedirect.com
SCIENCE DIRECT®
Polymer 45 (2004) 3877–3883
polymer
www.elsevier.com/locate/polymer

A Monte Carlo simulation of coarse-grained poly(silylenemethylene) and poly(dimethylsilylenemethylene) melts

Donghai Chen[a], Wayne L. Mattice[b,*]

[a]*Department of Natural Science, Malone College, Canton, Ohio 44709, USA*
[b]*Institute of Polymer Science, The University of Akron, Akron, Ohio 44325-3909, USA*

Received 21 March 2003; received in revised form 20 January 2004; accepted 20 January 2004

Abstract

Dense melts of coarse-grained representations of poly(silylenemethylene) (PSM) and poly(dimethylsilylenemethylene) (PDMSM) have been simulated at 373 K. The PSM melt has very little structure, and the individual chains have conformations in good agreement with the prediction from the rotational isomeric state (RIS) model for the single chain. For PDMSM, however, the melt is much more strongly structured, and the individual chains have mean square dimensions 40% higher than the ones predicted by the RIS model for the single chain. Intermolecular packing interactions in the structured PDMSM melt are accompanied by expansion of individual chains.

Keywords: Pair correlation functions; Poly(dimethylsilylenemethylene); Poly(silylenemethylene)

1. Introduction

The widespread use of polymeric hydrocarbons has prompted extensive simulations, for example [1–10], of these systems as amorphous materials at bulk density. Often the objective is insight into the molecular origin of important macroscopic properties of the material, such as the glass transition temperature of the polymer. Other objectives are the behavior of additives in the material, such as the diffusion coefficients of gaseous penetrants through the polymer [11].

Although less common, there is also interest in a related class of polymers in which some of the carbon atoms are replaced by silicon atoms [12–17]. Sometimes this replacement is achieved such that each C–C bond is replaced by a longer C–Si bond. Starting from two common structurally simple aliphatic polymeric hydrocarbons in which stereochemical composition is not an issue, namely polyethylene (PE) and polyisobutylene (PIB), these counterparts are poly(silylenemethylene) (PSM) and poly(dimethylsilylenemethylene) (PDMSM) [12–15]. The replacement of the shorter (0.154 nm) C–C bond by the longer (0.189 nm) C–Si bond tends to weaken the short-range intramolecular interactions in the chains. Therefore the preference for the trans state, which is well-known in PE [18], is weakened in PSM [19]. Similarly, the splitting of the trans and gauche states in PIB and poly(vinylidene chloride) [20] is weakened in PDMSM [13,14,19]. PDMSM is of special interest because its measured unperturbed dimensions [12] are reported to be significantly larger than the results predicted by application of the rotational isomeric state (RIS) model [13].

The previous modeling of PSM and PDMSM has focused on the analysis of RIS models [21] of unperturbed chains [13,14,19]. Here the RIS models are incorporated into simulations of dense melts of these two polymers, using a method that bridges between coarse-grained and atomistically detailed models of the system [10,22]. The dimensions of PSM in the weakly structured melt are in excellent agreement with the prediction from the RIS model. In contrast, the mean square dimensions for PDMSM in its strongly structured melt are about 40% larger than the prediction from the RIS model of the single chain.

2. Simulation method

The atomistically detailed chains are placed on a diamond lattice with a step length given by the length of

* Corresponding author. Tel.: +1-330-972-5128; fax: +1-330-972-5396.
E-mail address: wlm@polymer.uakron.edu (W.L. Mattice).

0032-3861/$ - see front matter © 2004 Elsevier Ltd. All rights reserved.
doi:10.1016/j.polymer.2004.01.077

the C–Si bond, 0.189 nm [16]. Coarse-graining then eliminates all atoms except the silicon atoms, and also eliminates alternate sites on the diamond lattice. The coarse-grained system is represented on a lattice with $10i^2 + 2$ sites in shell i and a step length of 0.3086 nm [23]. Each coarse-grained monomer is represented by a single bead, placed at the coordinates of the silicon atom.

Two types of energies are used in the Metropolis Monte Carlo simulation. Short-range intramolecular interactions influence the distribution of end-to-end distances for a chain and all of its subchains [24]. The intermolecular interactions and long-range intramolecular interactions are represented by a discretized, multi-shell representation of a Lennard–Jones (LJ) potential energy function [25].

The RIS model [21] is used for the short-range intramolecular interactions. The first- and second-order interactions in the model described recently [19] for PSM and the model of Ko and Mark for PDMSM [13] are incorporated into statistical weight matrices for the Si–Si coarse-grained bonds of length 0.3086 nm. The energies of the short-range interactions in the atomistically detailed models are listed in Table 1, along with the energies of the corresponding interactions in RIS models for PE [26] and PIB [27]. For poly(CH_2–XH_2), the interactions denoted by E_σ and E_ω are both weakened when X is changed from C to Si, due to the lengthening of the C–X bond. These changes cause the characteristic ratio, C, for the mean square unperturbed end-to-end distance, $\langle r^2\rangle_0/nl^2$, to decrease to 4.2 at 373 K when this substitution is made, because the fraction of bonds in the trans state has fallen to 0.47, in response to the weakening of the short-range interactions. At the same temperature, the RIS model for PDMSM specifies a C of 3.7, with 44% of the bonds in the trans state. Thus the RIS models for both silicon-containing chains have C's within 8% of 4.0 and a population of trans states within 5% of 0.45.

The long-range interactions are represented by a discretized version of the expression for the second virial coefficient of a non-ideal gas using the Mayer f function. This discretization insures that the continuous LJ function and its discretized counterpart specify the same value of the second virial coefficient for this pair-wise interaction of beads [25]. Since pertinent LJ parameters for the CH_2–SiH_2 and CH_2–$Si(CH_3)_2$ units were not found in the literature, the necessary parameters were estimated in this work, using two molecules of CH_3SiH_3 for PSM and two molecules of $CH_3Si(CH_3)_2H$ for PDMSM. With the aid of Cerius[2] version 4.0 from Accelrys, Inc., and the Universal 1.02 force field therein, the orientationally averaged intermolecular interaction of pairs of similar molecules was calculated as a function of the separation of their centers of mass. The orientational averaging was achieved by the following method: (1) the center of mass of one monomer was fixed at the origin of a Cartesian coordinate system, and the center of mass of the other monomer was placed at a distance r in the positive direction along the Z axis. (2) Three different orientations are used for the C–Si bond of the monomer at the origin: along the Z axis, with the Si pointed toward the second monomer; along the Z axis, with the Si pointed away from the second monomer; along the Y axis. (3) For each orientation of the first monomer, several different initial orientations of the second monomer were selected and then modified by rotations about the X, Y, and Z axes. (4) The numbers of initial orientations, and the numbers of modifications produced by rotations about the X, Y, and Z axes, were chosen by test calculations at different values of r. The number of test configurations was continually expanded until there was no longer any significant change in the orientationally averaged energy. The orientationally averaged energies as a function of r were then fitted to a LJ potential.

$$V(r) = -4\varepsilon[(\sigma_{LJ}/r)^6 - (\sigma_{LJ}/r)^{12}] \quad (1)$$

The method was tested using two molecules of ethane. The fit to the LJ potential, Fig. 1, yields $\sigma_{LJ} = 0.456$ nm and $\varepsilon/k = 218.9$ K, which are in reasonable agreement with literature values of $\sigma_{LJ} = 0.444$ nm and $\varepsilon/k = 215.7$ K from Reid et al. [28] and $\sigma_{LJ} = 0.478$ nm and $\varepsilon/k = 216.12$ K of Cuadros et al. [29]. The fits produced by application of the same method to the silicon-containing molecules are depicted in Fig. 2. The parameters deduced from these fits, and similar application to isobutane, are presented in Table 2.

The shell energies, u_i, for the first five shells for the

Table 1
First- and second order interaction energies (kJ/mol) for poly(XR_2–CH_2)

X, R	Bond	E_σ	E_τ	E_ψ	E_ω	Ref.
Si, H	C–X	0.7	0.1	0.3	3.0	19
Si, H	X–C	0.7	0.5	−0.4	4.6	19
C, H	C–X, X–C	2.1	0	0	8.4	26
Si, CH_3	C–X	0	0	0	0.8	13
Si, CH_3	X–C	0	0	0	∞	13
C, CH_3	C–X	0.2–0.8	0	0	0	27
C, CH_3	X–C	0.2–0.8	0	6.3–8.4	∞	27

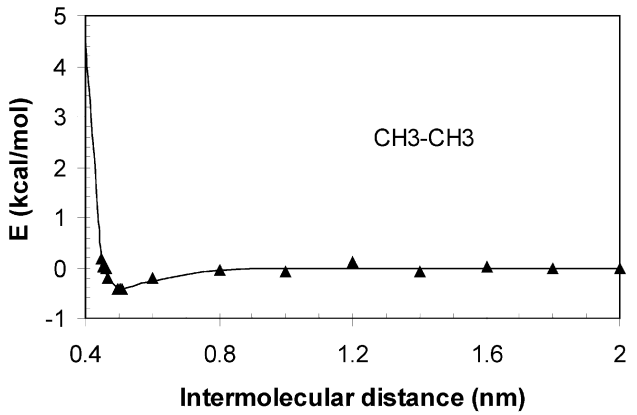

Fig. 1. Fit of the orientationally averaged energies of two molecules of ethane to a Lennard–Jones potential.

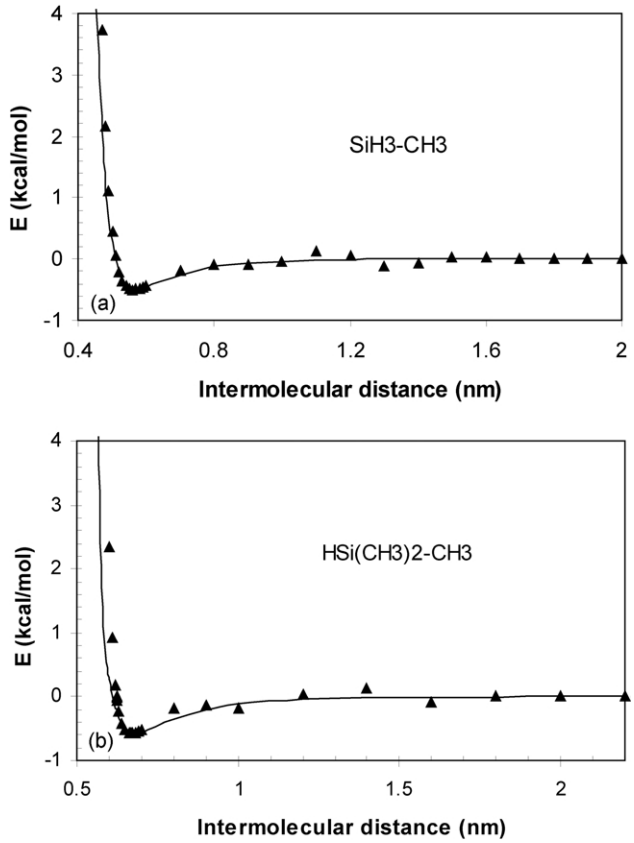

Fig. 2. Fit to a Lennard–Jones potential of the orientationally averaged energies of two molecules of (a) CH_3SiH_3 and (b) $CH_3Si(CH_3)_2H$.

silicon-containing molecules, evaluated with Cho's method [25] at 373 K, are listed in Table 3. The first shell has a strongly positive energy because the step length on the high coordination lattice is smaller than σ_{LJ}. The most negative energy is u_3. Higher shells also have negative energies, but they are weaker than the energy in the third shell. The energies for the first three shells were used in the simulations reported in this work.

Both single-bead moves [22] and multiple bead pivot moves [30] were applied in the simulations. One Monte Carlo Step (MCS) is defined as the simulation length when every bead in the system has attempted one move, on average. The Metropolis rule was applied to determine whether or not the move is made. Moves that produce double occupancy or collapses [22] are disallowed.

Table 2
Lennard–Jones parameters deduced for three pairs of molecules by the method described in this work

Molecule	X	σ_{LJ} (nm)	ε/k (K)
CH_3XH_3	C	0.456	218.9
CH_3XH_3	Si	0.501	252.6
$CH_3X(CH_3)_2H$	C	0.5278	330.1
$CH_3X(CH_3)_2H$	Si	0.61	288.9

The data for isobutane is from Reid et al. [28].

Table 3
Shell energies (kJ/mol) at 373 K for PSM and PDMSM

Shell	PSM	PDMSM
1	9.071	19.188
2	−0.600	1.268
3	−0.653	−1.360
4	−0.133	−0.476
5	−0.034	−0.127

3. Plateau density of free-standing thin films

The natural bulk densities for amorphous systems constructed from the coarse-grained chains were determined by equilibrating replicas of free-standing thin films that were sufficiently thick to have an internal plateau density. The thin films were generated by the method of Misra et al. [31] as implemented on the discrete space of a high coordination lattice [32]. For PSM (or PDMSM) the system had 45 (or 25) independent coarse-grained parent chains, each represented by 20 beads. The chains reverse-map to $Si_{20}C_{20}H_{82}$ and $Si_{20}C_{61}H_{164}$, respectively. After pre-equilibration in a periodic box with 16 steps of length 0.3086 nm in each direction, the periodicity along the Z axis was increased to 48 steps so that the chains no longer interact with their images in the Z direction. After about 3 million additional MCS, the system settles into a free-standing thin film with a density profile that no longer changes with simulation time.

The density profiles, (z), for PSM at 373 K is depicted in Fig. 3a, using bins of width 0.2 nm in the analysis. The figure also shows the fits of these profiles to the equation proposed by Helfand and Tagami for the interface in immiscible binary blends [33,34].

$$\rho(z) = (\rho_0/2)\{1 - \tanh[(z - z_0)/\xi]\} \quad (2)$$

The plateau density is denoted by ρ_0, and z_0 and ξ define the mean position and thickness, respectively, of the surface region. The parameters used in the simulation specify a bulk density of 1.10 g/cm^3 at 373 K. Similar simulations for PDMSM, depicted in Fig. 3b, specify a bulk density of 1.05 g/cm^3 at 373 K. The two systems have densities slightly above 1 g/cm^3. This density is slightly higher than the results expected for analogous hydrocarbons at the same temperature, because the silicon atom is heavier than the carbon atom. PSM has a higher bulk density than PDMSM because it contains a higher weight fraction of silicon.

4. Equilibration: mobility of the chains in their melts

The sizes of the bulk systems studied at 373 K are given in Table 4. The notations (s) and (l) differentiate simulations with shorter and longer chains, respectively, at the same density.

The simulation time required for equilibration of the conformations of the chains in the melts was investigated by

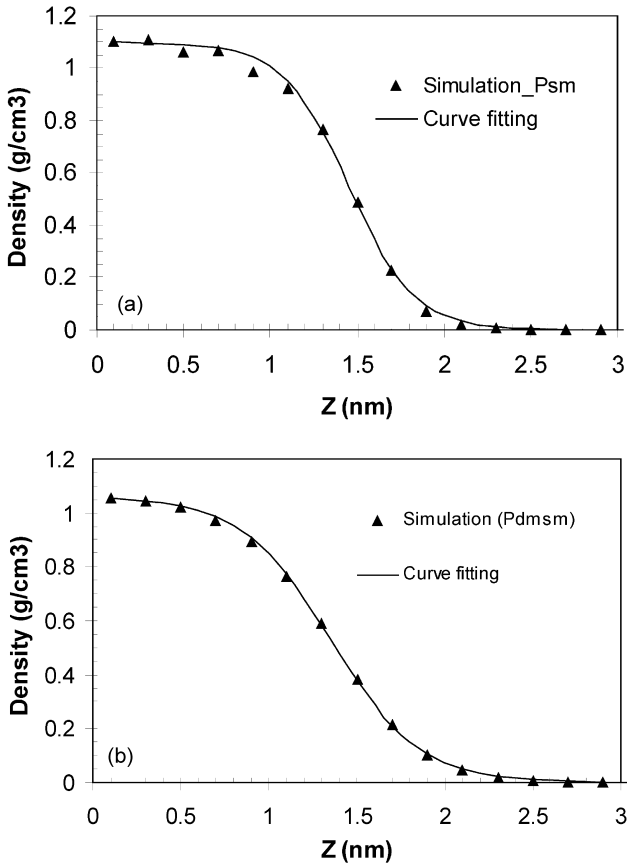

Fig. 3. Density profiles normal to the surface for thin films of (a) PSM and (b) PDMSM at 373, along with the hyperbolic tangent fit to each profile. The midplane is at $z = 0$.

finding the characteristic time, τ_d, for decay of the orientation autocorrelation functions (OACF) defined with the end-to-end vector, $\langle \mathbf{r}(t)\cdot\mathbf{r}(0)\rangle/\langle r^2\rangle$, and the coarse-grained bond vector of length 0.3086 nm, $\langle \mathbf{m}(t)\cdot\mathbf{m}(0)\rangle/m^2$. These OACF are depicted in Fig. 4 for the simulation PSM(l). Complete decay of both OACF is obtained in 20 million MCS. The values of τ_d are evaluated by integrating the area under the curves. These τ_d, as well as similar times obtained from PSM(s), PDMSM(s), and PDMSM(l), are presented in Table 5. The longest τ_d was obtained for the OACFs depicted in Fig. 4.

Based on the numbers in Table 5, simulations of 3 million MCS were performed for the systems with the shorter chains. The static properties were evaluated from the

Table 4
Parameters in the bulk simulations of PSM and PDMSM at 373 K in three-dimensional periodic boxes with L steps in each direction

Property	PSM(s)	PSM(l)	PDMSM(s)	PDMSM(l)
Beads per chain	20	50	20	50
Number of chains	52	50	31	29
L	15	20	15	20
ρ (g/cm^3)	1.10	1.10	1.05	1.05
Site occupancy	0.31	0.31	0.18	0.18

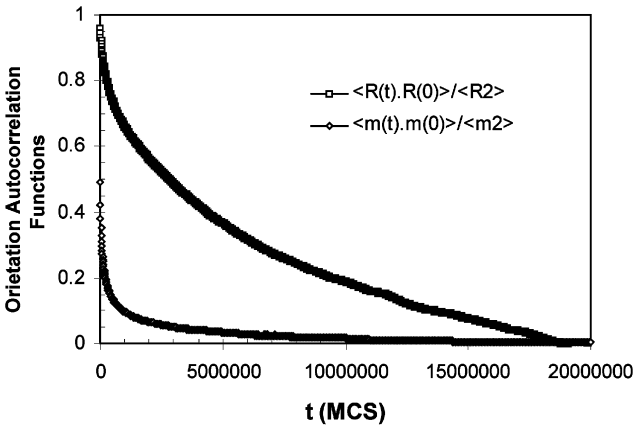

Fig. 4. Decay of the orientation autocorrelation functions defined by the end-to-end vector and coarse-grained bond vector in the PSM(l) simulation at 373 K.

configurations during the last 2 million MCS. For the longer chains, the simulations were conducted for 40 million MCS (or 22 million MCS) for PSM(l) (or for PDMSM(l)). The static properties were evaluated from the configurations during the last 4 million MCS of these simulations.

5. Static properties

All of the simulations at 373 K find the fraction of the internal C–Si bonds in trans states is in the range 0.39–0.40. These numbers are slightly smaller than the expectation (0.47 for PSM, 0.44 for PDMSM) from the RIS model [19].

The root-mean-square radii of gyration, $\langle s^2\rangle^{1/2}$, of the shorter chains are 0.82 and 0.93 nm for PSM and PDMSM. For the longer chains, the respective $\langle s^2\rangle^{1/2}$, are 1.42 and 1.68 nm. The ratio of these numbers to the length of a side of the periodic box is in the range 0.18–0.27, which suggests artificial imaging effects from the periodic boundary conditions should be negligible.

The four simulations yield values of $\langle r^2\rangle/\langle s^2\rangle$ in the range 6.35–6.63. These results are consistent with expectation, because random coils with fewer than 100 bond often have values of this ratio that are slightly larger than 6. This departure of the ratio from the infinite chain limit of 6 arises because the finite chain length corrections are stronger in $\langle s^2\rangle$ than in $\langle r^2\rangle$.

The values of C for the longer chains are 3.6 for PSM and

Table 5
τ_d (in millions of MCS) for decay of the orientation autocorrelation functions in the melts at 373 K

Simulation	OACF defined with **r**	OACF defined with **m**
PSM(s)	0.151	0.031
PSM(l)	4.84	0.566
PDMSM(s)	0.251	0.084
PDMSM(l)	2.05	0.517

5.1 for PDMSM. The RIS model predicts asymptotic limits of 4.15 and 3.67. The agreement between simulation and the RIS model is quite good for PSM. However, for PDMSM the simulation gives a value of C nearly 40% larger than the asymptotic limit from the RIS model. It is intriguing to note that Ko and Mark also found the experimental C for PDMSM, based on measurements performed in dilute solution in cyclohexane [12], was significantly larger than the result predicted by their RIS model [13]. Their experimental value of C, 5.32 [12], is within 5% of the value obtained in the present work in the melt simulation denoted PDMSM(l).

The local intermolecular packing in the melts was studied using the intermolecular pair correlation function (PCF). This pair correlation function evaluates the probability of finding a particle A in a spherical shell about another particle A, in comparison with the result expected from an ideal gas formed from the same particles at the same overall density. On the discrete space of the high coordination lattice, the PCF for shell i is defined as [35]

$$g_{AA}(i) = \langle n_{AA}(i) \rangle / (10^2 i + 2) V_A \quad (3)$$

The numerator is the ensemble average of the number occupancy of A in the ith shell about another A, $10i^2 + 2$ is the number of cells in shell i, and V_A is the volume fraction of A in the system.

The PCF for PSM, Fig. 5a, is rather uninteresting, being characterized primarily by the avoidance of a first-shell interaction. The first maximum, seen in the third shell, is weaker than the first maximum in the PCF for the simulation of PE melts by a similar method. The reduction in the intermolecular structure in the melt when moving from PE to PSM may be attributed to the fact that the silicon-containing polymer has a weaker preference for trans states, with p_t of about 0.4, in comparison with a p_t of about 0.6 for a PE melt at the same temperature.

The PCF of PDMSM, Fig. 5b, shows significantly more structure than the melt of PSM, Fig. 5a. The PCF of PDMSM exhibits easily detected maxima at the third and sixth shells. If the rather strong preferences for specific intermolecular packing of PDMSM in its melt modify the preferences exerted by short-range intramolecular conformations for specific local conformations, it would be possible for the C of the chains in the melt to be different from the C determined solely by the short-range intramolecular interactions. The direction of the discrepancy between measured [12] and RIS [13,19] values of C for PDMSM implies that the formation of the intermolecular structure in evidence in the PCF in Fig. 5b is achieved by extension of the chains.

Melts of coarse-grained chains of PIB have not been simulated on high coordination lattices of the type used in this work, making it difficult to directly compare the PCF in Fig. 5b with the expectation for coarse-grained PIB from this type of simulation. However, pair correlation functions

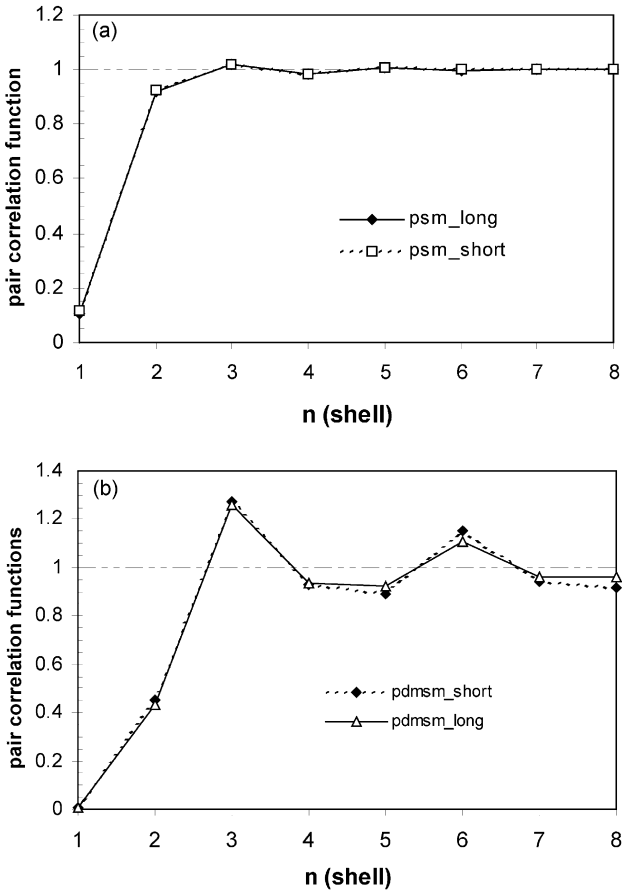

Fig. 5. Intermolecular pair correlation function at 373 K, as a function of shell number, for melts of (a) PSM and (b) PDMSM.

from simulations of atomistically detailed models of PE melts and for the backbone carbon atoms in PIB melts in continuous space provide no indication that the PIB melt is more highly structured that the PE melt [2]. Indeed, it is less structured instead. The observation of greater structure in the PDMSM melt than in the PSM melt does not have a precedent in the analogous polymeric hydrocarbons.

Table 6 presents the cohesive energy densities calculated from the simulations of the melts and the surface energies calculated from the simulations of the free-standing thin films. The surface energies are in the general range that might be expected for similar hydrocarbons, in the range of 27–32 erg/cm^2 at temperatures of 20–35 °C [36,37]. The most interesting numbers in this table are the low cohesive energies for PDMSM. The values cited in the literature for PE and PIB at 20–35 °C are in the range 61–63 cal/cm^3

Table 6
Cohesive energie density (cal/cm^3) and surface energy (erg/cm^2) at 373 K

Simulation	Cohesive energy density	Surface energy
PSM(s)	53	31
PSM(l)	53	39
PDMSM(s)	34	30
PDMSM(l)	32	31

[36–37], which are nearly twice as large as the results from the simulation for PDMSM. This comparison suggests that the strong preferences for specific intermolecular structure, see in Fig. 5b, are more likely to originate from repulsive interactions between the chains, rather than specific attractive interactions.

If one seeks an explanation in the shell energies, Table 3, for the differences in behavior of PSM and PDMSM in their melts, attention may first be drawn to the fact the largest attraction is found in u_3 for PDMSM. This negative u_3 certainly contributes to the PDMCM melt having a higher maximum in the PCF at shell 3 than does the PSM melt. It does not, however, explain why PDMSM has a lower cohesive energy density than PSM. Attention must be directed to u_2 in order to understand the cohesive energy densities. The relatively small cross-section of the PSM chain, as reflected in its value for σ_{LJ}, easily accommodates a second shell interaction, as well as a third shell interaction. Indeed, there is very little energetic discrimination between u_2 and u_3 for PSM. With its larger cross-section (larger σ_{LJ}), u_2 for PDMSM is positive and signifies a significant repulsion in the second shell interaction. The change in sign upon proceeding from u_2 to u_3 contributes strongly to the structure seen in the PCF for PDMSM, and the near equivalence of u_2 and u_3 for PSM leads to comparatively little structure in the PSM melt. Since the overall density of the systems demands that some second-shell interactions must be present, the cohesive energy is smaller for PDMSM that for PSM. Apparently the best possible avoidance of the repulsive second shell interaction in the dense PDMSM melts is achieved by a slight expansion of the chains beyond the dimensions expected from the single-chain RIS model. Thus it is the interplay of the preferred density of the system and the values of u_2 and u_3 that accounts for the differences in the behavior of the PSM and PDMSM melts in the simulations.

6. Conclusions

Simulations of PSM, with repeating sequence CH_2-SiX_2, X = H, suggest that the melt is a rather structureless material. The intermolecular PCF shows less structure than does PE under the same conditions. The intermolecular structure in the PSM melt is confined to distances less than 1 nm. The cohesive energy density and surface energy are close to the expectations for a polymeric hydrocarbon. The mean square dimensions of the chains in the melt are very close to the expectation from the RIS model.

Similar simulations of PDMSM, with repeating sequence of CH_2-SiX_2, X = CH_3, present a more interesting picture. In agreement with observations many years ago by Ko and Mark in their comparison of experiments and RIS calculations, the PDMSM chains are significantly more extended in experiment than one would expect based on the RIS model [13]. The dimensions of PDMSM in the present simulations of the melt are in excellent agreement with the experimental measurements in dilute solution in cyclohexane that were reported by Ko and Mark [12]. Ko and Mark suggested that the nonequivalence in the two types of bond angles in the backbone of the polymer may have contributed to the difference in the dimensions obtained in their experiments and RIS models. Although such an explanation might hold for their measurements in dilute solution, it could not explain the results in the present simulation, because the present simulations enforce exactly the same bond angles (tetrahedral) for all backbone bonds. The intermolecular PCF in the present simulations of the melt exhibits two easily detected maxima, which indicate the presence of structure on a distance scale extending well over 1 nm. The cohesive energy density is unusually low, suggesting that repulsive interactions may contribute to the structure in the melt. The same interactions may produce expansion of individual chains, causing the measured dimensions in the melt to exceed the dimensions predicted by the RIS model.

Elaboration of the structure of the repeating unit to CH_2-SiXY, X = CH_3, Y = $O(CH2)_xOC_6H_4C_6H_5$ produces a polymer with very strong intermolecular structure at a temperature slightly below 373 K, as shown by the development of liquid crystalline phases [17]. The present work demonstrated the tendency for formation of structure in the melt can be detected in the simpler polymer, with repeating sequence CH_2-SiX_2, X = CH_3.

Acknowledgements

This research was supported by the Collaborative Center in Polymer Photonics, funded by the Air Force Office of Sciencific Research and Wright Patterson Airforce Base, and by National Science Foundation grant DMR 0098321. One of the authors (D. C.) would like to thank Malone College for granting him the sabbatical leave for this research opportunity. He also thanks Dr G. Xu and Dr C. Helfer for their help on using programs and software and for many useful discussions during his stay at The University of Akron.

References

[1] Theodorou DN, Suter UW. Detailed molecular structure of a vinyl polymer glass. Macromolecules 1985;18:1467.
[2] Boyd RH, Pant PVK. Molecular packing and diffusion in polyisobutylene. Macromolecules 1991;24:6325.
[3] Paul W, Binder K, Heermann DW, Kremer K. Dynamics of polymer solutions and melts. Reptation prediction and scaling relaxation times. J Chem Phys 1991;95:7726.
[4] Pant PVK, Han J, Smith GC, Boyd RH. A molecular dynamics simulation of polyethylene. J Chem Phys 1993;99:597.
[5] Smith GD, Yoon DY, Zhu W, Ediger MD. Comparison of equilibrium

and dynamics properties of polymethylene melts of n-$C_{44}H_{90}$ chains from simulations and experiments. Macromolecules 1994;27:5563.
[6] Schweizer KS, David EF, Singh C, Curro JG, Rajasekaran JJ. Structure–property correlations of atomistic and coarse-grained models of polymer melts. Macromolecules 1995;28:1528.
[7] Maranas JK, Kumar SK, Debenedetti PG, Graessley WW, Mondello M, Grest GS. Liquid structure, thermodynamics, and mixing behavior of saturated hydrocarbon polymer. 2. Pair distribution functions and the regularity of mixing. Macromolecules 1998;31:6998.
[8] Antoniadis SJ, Samara CT, Theodorou DN. Effect of tacticity on the molecular dynamics of polypropylene melts. Macromolecules 1999; 32:8635.
[9] Clancy TC, Pütz M, Weinhold JD, Curro JG, Mattice WL. Mixing of isotactic and syndiotactic polypropylenes in the melt. Macromolecules 2000;33:9452.
[10] Baschnagel J, Binder K, Doruker P, Gusev AA, Hahn O, Kremer K, Mattice WL, Müller-Plathe F, Murat M, Paul W, Sanatos S, Suter UW, Tries V. Bridging the gap between atomistic and coarse-grained models: status and perspectives. Adv Polym Sci 2000;152:41.
[11] Han J, Boyd RH. Small-molecule penetrant diffusion in hydrocarbon polymers as studied by molecular dynamics simulation. Macromolecules 1994;27:5365.
[12] Ko JH, Mark JE. Configuration-dependent properties of poly(dimethylsilmethylene) chains. I. Experimental results. Macromolecules 1975;8:869.
[13] Ko JH, Mark JE. Configuration-dependent properties of poly(dimethylsilmethylene) chains. II. Correlation of theory and experiment. Macromolecules 1975;8:874.
[14] Sundararajan PR. Conformational aspects of poly(dimethylsilaethylene), an analog of polyisobutylene. Comput Polym Sci 1991;1:18.
[15] Tsao MW, Pfeifer KH, Rabolt JF, Holt DB, Farmer BL, Interrante LV, Shen Q. Studies of the solid-state conformation of polysilmethylene: an organic/inorganic hybrid polymer with an alternate C/Si backbone. Macromolecules 1996;26:7130.
[16] Park SY, Interrante V, Farmer BL. The structure of poly(di-*n*-propylsilylenemethylene). Polymer 2001;42:4253.
[17] Park SY, Zhang T, Interrante LV, Farmer GL. Structures of side chain liquid crystalline poly(silylenemethylene)s. Macromolecules 2002; 35:2776.
[18] Abe A, Jernigan RL, Flory PJ. Conformational energies of *n*-alkanes and the random configuration of high homologs including polymethylene. J Am Chem Soc 1966;88:631.
[19] Helfer CA, Mattice WL, Chen D. Substituted poly(silylenemethylene)s with short range interactions that induce a preference for the same local conformation in unperturbed atactic, isotactic, and syndiotactic chains. Polymer 2004;45:1297.
[20] Boyd RH, Kesner L. Conformation properties of polar polymers. II. Poly(vinylidene chloride). J Polym Sci, Polym Phys Ed 1981;19:393.
[21] Flory PJ. Foundation of rotational isomeric state theory and general method for generating configuration averages. Macromolecules 1974; 7:381.
[22] Doruker P, Mattice WL. Reverse mapping of coarse-grained polyethylene chains from the second nearest neighbor diamond lattice to an atomsitic model in continuous space. Macromolecules 1997;30:5520.
[23] Rapold RF, Mattice WL. New high coordination lattice model for rotational isomeric state (RIS) polymer chains. J Chem Soc Faraday Trans 1995;91:2435.
[24] Rapold RF, Mattice WL. Introduction of short and long range energies to simulation of real chains on the 2nd lattice. Macromolecules 1996; 29:2457.
[25] Cho J, Mattice WL. Estimation of long range interaction in coarse-grained rotational isomeric state polyethylene chains on a high coordination lattice. Macromolecules 1997;30:637.
[26] Jernigan RL, Flory PJ. Configurational correlation in chain molecules. J Chem Phys 1969;50:4165.
[27] Liberman MH, DeBolt LC, Flory PJ. Optical anisotropy of polyisobutylene: strain birefringence. J Polym Sci, Polym Phys 1974;12:187.
[28] Reid RC, Prausnitz JM, Poling BE. The properties of gases and liquids, 4th ed. New York: McGraw-Hill; 1987. p. 773.
[29] Cuadros F, Cachadina I, Ahamuda W. Determination of Lennard–Jones interaction parameters using a new procedure. Mol Engng 1996; 6:319.
[30] Clancy TC, Mattice WL. Rotational isomeric state chains on a high coordination lattice: dynamic Monte Carlo algorithm details. J Chem Phys 2000;112:10049.
[31] Misra S, Fleming PD, Mattice WL. Structure and energy of thin films of poly(1,4-*cis*-butadiene). A new atomistic approach. J Comput-Aided Mater Des 1995;2:101.
[32] Doruker P, Mattice WL. Simulation of polethylene thin films on a high coordination lattice. Macromolecules 1998;31:1418.
[33] Helfand E, Tagami Y. Theory of the interface between immisicble polymers. II. J Chem Phys 1971;56:3592.
[34] Helfand E, Tagami Y. Theory of the interface between immiscible polymers. J Chem Phys 1972;57:1812.
[35] Xu G, Mattice WL. Study on structure formation of short polyethylene chains via dynamic Monte Carlo simulation. Comput Theor Polym Sci 2001;11:405.
[36] Wu S. Surface and interfacial tensions of polymer melts I. Polyethylene, polyisobutylene, and polyvinyl acetate. J Colloid Interface Sci 1969;31:153.
[37] Mangaraj D, Bhatnagas SK, Rath SB. Cohesive-Energy-densities of high polymers Part III. Estimation of C.E.D. by viscosity measurements. Makromol Chem 1963;67:75.